Inorganica Chimica Acta 424 (2015) 63–74

Contents lists available at ScienceDirect

Inorganica Chimica Acta

journal homepage: www.elsevier.com/locate/ica

Review

Dimolybdenum dimers spaced by phenylene groups: The experimental models for study of electronic coupling

Hao Lei [a], Xuan Xiao [b], Miao Meng [a], Tao Cheng [a], Yao Shu [a], Ying Ning Tan [a], Chun Y. Liu [a,b,*]

[a] Department of Chemistry, Jinan University, 601 Huang-Pu Avenue West, Guangzhou 510632, China
[b] Department of Chemistry, Tongji University, 1239 Siping Road, Shanghai 200092, China

ARTICLE INFO

Article history:
Received 15 June 2014
Received in revised form 17 September 2014
Accepted 18 September 2014
Available online 16 October 2014

Keywords:
Metal–metal bond
Electron transfer
Electronic coupling
Hush model
Mixed-valance compound

ABSTRACT

This account reviews our recent investigation on the electronic coupling and intramolecular electron transfer in D–B–A systems constructed by employing covalently bonded [Mo_2] units as the electron donor (D) and acceptor (A) and phenylene groups as the bridges (B). In these complexes, the δ electrons are transferring from the donor to the acceptor and thus, exclusively responsible for the electrochemical and optical behaviors. The unique electronic structures for the donor and acceptor sites as well as the D–B–A molecules make them excellent experimental models for validating and refining the existing electronic coupling and electron transfer theories. By designed syntheses of the complex systems, the impact of coordinating atoms and length of bridging ligands and electronic property of the ancillary ligands on the donor–acceptor interaction have been examined by means of electrochemical, spectroscopic, magnetic techniques and theoretic calculations. The widely accepted Hush vibronic model and the latest CNS superexchange formalism have been employed to determine the electronic coupling matrix elements (H), which yield remarkably consistent results. By modulation of the structural variables, the electronic coupling interaction in the mixed-valence complexes varies from weakly to moderately strong coupling; the MV systems span a transition from Class II to the Class II/III borderline in terms of Robin-Day's classification. On this basis, the intramolecular electron transfer kinetics has been studied under the Marcus–Hush semi-classical framework. The adiabatic electron transfer rate constants are determined in the range of 10^8–10^{12} s^{-1}, depending on the nature of bridge. The results also offer new mechanistic insights into electron transfer theory, as both electron-hopping and hole-hopping pathways are confirmed to be effective for certain compounds.

Hao Lei *received his B.S. degree in chemistry from Peking University in 2006 and his Ph.D. from University of California-Davis in 2011, where he worked under the supervision of Professor Philip P. Power. After postdoctoral research at University of Illinois and University of Maryland, he came back to China to join the faculty at Jinan University. His research interests focus on the synthesis and reactivity of earth-abundant metal complexes with novel bonding motifs.*

* Corresponding author at: Department of Chemistry, Jinan University, 601 Huang-Pu Avenue West, Guangzhou 510632, China. Tel.: +86 020 85222191; fax: +86 020 85220223.
E-mail address: tcyliu@jnu.edu.cn (C.Y. Liu).

http://dx.doi.org/10.1016/j.ica.2014.09.039
0020-1693/

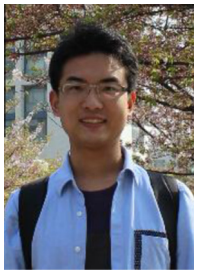

Xuan Xiao *received his B.S. degree in chemistry from Tongji University in 2010. He is currently pursuing his Ph.D. degree under Prof. Chun Y. Liu's supervision. His research interests are mainly the development of experimental systems for the study of electronic coupling and intramolecular electron transfer.*

Miao Meng *obtained her M.S. degree from Sun Yat-sen University in 2009. Subsequently she joined the laboratory of Prof. Chun Y. Liu at Jinan University. Her research interests include transition metal complexes, mixed-valence chemistry and intramolecular charge transfer.*

Tao Cheng *is a graduate student with Prof. Chun Y. Liu at Jinan University. His present research objective is to study intramolecular electron transfer using experimental models constructed by quadruply bonded dimolybdenum units.*

Yao Shu *obtained his M.S. degree under Prof. Chun Y. Liu's supervision at Jinan University in 2014. In his research work, he studied electronic coupling and electron transfer in* Mo_2 *dimers with various bridging ligands.*

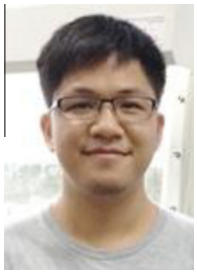

Ying Ning Tan *is currently a graduate student in Prof. Chun Y. Liu's group at Jinan University. His research focuses on experimental and theoretical studies on compounds having multiple metal–metal bonds.*

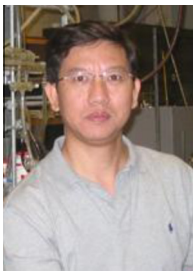

Chun Yuan Liu *studied chemistry at Jinan University and received his M.S. degree in 1988. Then he worked, as a faculty member, in the department of chemistry at Xiangtan Normal College. From 1996 to 1999, he was a researcher in Daryle H. Busch's group at the University of Kansas. Afterwards, he joined F. Albert Cotton's group at Texas A&M University, where he obtained his Ph.D. in 2005. After finishing his postdoctoral work with Cotton in 2007, Liu began his professorship at Tongji University. He moved to Jinan University in 2011 and presently chairs the department of chemistry at this university. His research interests include metal-metal bonds, mixed-valency, electronic coupling and electron transfer.*

Contents

1. Introduction

For decades, great efforts have been made in understanding and controlling electron transfer (ET) reactions that are ubiquitous in chemical [1–4] and biological systems [5,6]. Exploration in this realm has been relying on the establishment of theoretical frameworks and development of synthetic models, thus, generating an interplaying field for experimental and theoretic scientists.

In the traditional two-state model, the energies of ET reactant and product are represented by two crossing parabolic wells, which forms the diabatic energy surfaces in a plot of energy versus reaction coordinate X [7]. Fig. 1A presents the electron transfer reaction in weakly coupled symmetrical systems, for which the free energy change (ΔG°) is zero. In an unsymmetrical system, however, the difference in energy between the reactant and product may be greater or less than zero, as shown in Fig. 1B for the case of $\Delta G^{\circ} > 0$. The effect of electronic interaction can be quantitatively described by a parameter, namely, electronic coupling matrix element (H_{ab}). As a result of electronic coupling, the adiabatic lower and upper states are separated by $2H_{ab}$ at $X = 0.5$. As the H_{ab} value increases, the activation energy (ΔG^{*}) decreases and the ET reaction is accelerated. Therefore, electronic coupling plays a critical role in controlling the adiabatic ET reaction.

Electronic coupling also determines the charge distribution over the entire molecule. Mixed-valence (MV) compounds in the type of donor-bridge-acceptor (D–B–A) can be categorized according to Robin-Day's scheme [8], that is, Class I, II and III. While Class I and Class III refer to the two extreme situations, i.e. fully localized and fully delocalized, respectively, Class II includes molecules where the charge are unequally distributed on the two sites due to the weak electronic interaction between them. In both theoretical and experimental aspects, it has been a challenging task to develop suitable complex models to describe the transition between charge localized and delocalized systems.

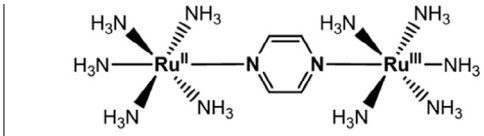

I

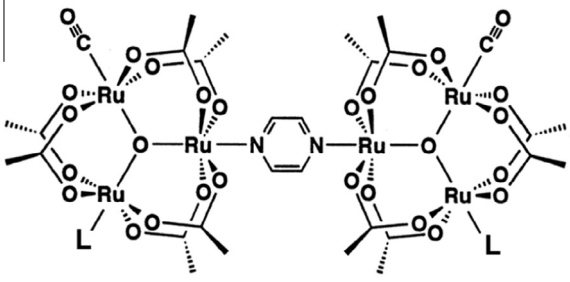

II

In experimental studies, MV coordination compound $[(NH_3)_5Ru(pyrazine)Ru(NH_3)_5]^{5+}$ (**I**), better known as the Creutz–Taube ion, is the first designed D–B–A metal complex model [9,10]. With this complex cation as the landmark, numerous binuclear $d^{5\text{-}6}$ metal complexes, produced by varying the metal centers, bridging ligand, ancillary ligands and coordination mode, have been synthesized

and studied with respect to electronic coupling [11–13]. Thereafter, bridged triruthenium clusters (**II**), Ru_3–Ru_3, have been intensively studied in terms of electronic coupling and intramolecular electron transfer, which further promoted better understanding of the related ET behaviors [14–16]. In addition, purely organic compounds have also been actively involved in this research since the 1990s [17,18].

Since Cotton's first report of metal–metal quadruple bond in $Re_2Cl_8^{2-}$ [19], innumerous quadruply bonded dimetal units with different metal/ligand combinations have been studied on the molecular and electronic structures. In 1990s, with the unique electronic configuration of a dimetal units M_2^{4+} (M = Mo, W), i.e., $\sigma^2\pi^4\delta^2$, Chisholm initiated the research of assembling two dimetal complex units by a bridging ligand (dicarboxylate in general) for the study of the intramolecular electronic coupling [20–22]. The first dicarboxylate bridged dimolybdenum dimer was structurally characterized by Cotton et al. [23], in which N-donor formamidinate anions were used as the ancillary ligands for the Mo_2 units. Later, the category of bridging ligands was further extended to diamidate and dithiodiamidate, and many other structural motifs with bridging groups fitting a pair of equatorial coordinating sites of the M_2 unit. Studies on various compounds of this type, carried out mainly by Cotton's and Chisholm's group, showed that the length, donor atoms, conjugation and conformation of the bridging ligand, impose a significant impact on the electronic communication between the two [M_2] units [23–25]. Recent work further shows that D–B–A systems constructed by [M_2] units and desirable bridging ligands are favorable experimental systems for the study of mixed-valency, electronic coupling and intramolecular electron transfer (Fig. 2).

By taking advantages of the unique molecular and electronic features for the molybdenum *dimers of dimers*, we have been focusing our research interest on mixed-valency, intramolecular electronic coupling and electron transfer. In this account we give a comparative overview of our recent work concerning such systems with various bridging and ancillary ligands. It is demonstrated that systematic chemical modification of the ligands offers some insights into the electron transfer properties and mechanisms for the complex systems. It is noteworthy that some related work on group 6 *dimers of dimers* compounds has been reviewed by Cotton [26], Chisholm [27,28] and Murillo [29].

2. The molecular systems concerned

All the dimolybdenum dimers that will be discussed are summarized in Table 1, with the common structure framework shown in Scheme 1, where *n* is the number of phenylene group in the bridge and E_1–E_4 represent the four coordinating atoms. Each of the Mo_2 units is supported by three diarylformamidinate (DArF) ligands. The most commonly used version of this type of ligands is that with *para*-methoxy group on the phenyl ring, i.e. *N,N′*-di(*p*-anisyl)formamidinate (DAniF) anion. Terephthalate bridged dimolybdenum dimer is one of the first synthesized molecules of this type (Table 1, entry 1). With similar molecular skeleton, a

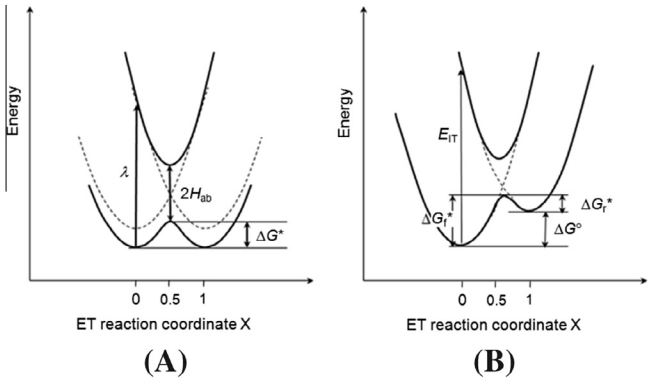

Fig. 1. Marcus–Hush potential energy surfaces for ET reactions, (A) for symmetrical intervalence (IV) systems ($\Delta G^\circ = 0$), and (B) for unsymmetrical IV systems ($\Delta G^\circ > 0$). The diabatic surfaces and adiabatic surfaces are presented by dotted and solid lines, respectively.

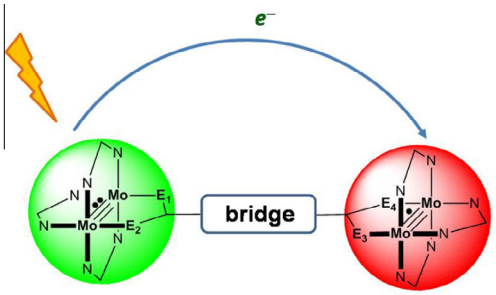

Fig. 2. Schematics showing the optical electron transfer process between two [Mo_2] units in the *dimers of dimers*. The donor (green) has a quadruply bonded dimolybdenum unit and the acceptor (red) has a single electron residing on the δ orbital.

Table 1
List of the molybdenum *dimers of dimers* discussed in this account.

Entry	Compd.	$(ph)_n$	E_1	E_2	E_3	E_4	R
1	**[O_2-$(ph)_1$-O_2]**	1	O	O	O	O	OCH_3
2	**[OS-$(ph)_1$-OS]**	1	O	S	O	S	OCH_3
3	**[S_2-$(ph)_1$-S_2]**	1	S	S	S	S	OCH_3
4	**[O_2-$(ph)_1$-S_2]**	1	O	O	S	S	OCH_3
5	**[O_2-$(ph)_2$-O_2]**	2	O	O	O	O	OCH_3
6	**[OS-$(ph)_2$-OS]**	2	O	S	O	S	OCH_3
7	**[S_2-$(ph)_2$-S_2]**	2	S	S	S	S	OCH_3
8	**[N_2-$(ph)_1$-N_2]**	1	NH	NH	NH	NH	OCH_3
9	**[NO-$(ph)_1$-NO]**	1	NH	O	NH	O	OCH_3
10	**[NS-$(ph)_1$-NS]**	1	NH	S	NH	S	OCH_3
11	**[O_2-$(ph)_1$-O_2]-CH_3**	1	O	O	O	O	CH_3
12	**[O_2-$(ph)_1$-O_2]-F**	1	O	O	O	O	F
13	**[O_2-$(ph)_1$-O_2]-Cl**	1	O	O	O	O	Cl
14	**[O_2-$(ph)_1$-O_2]-OCF_3**	1	O	O	O	O	OCF_3
15	**[O_2-$(ph)_1$-O_2]-CF_3**	1	O	O	O	O	CF_3

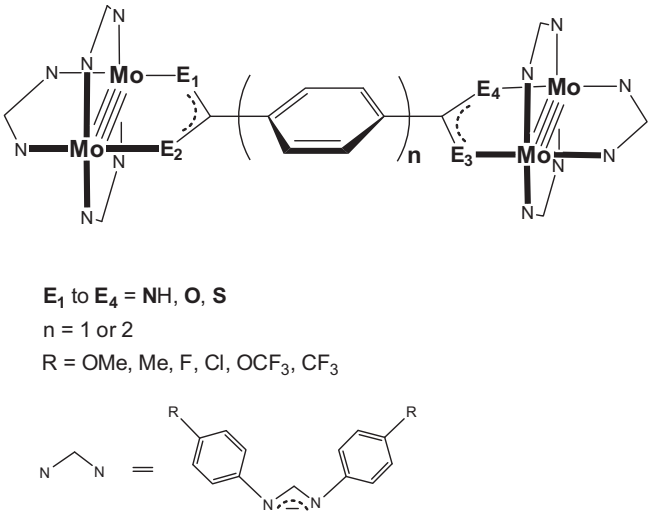

Scheme 1. A schematic representation of the dimolybdenum dimers discussed in this account.

series of analogues differing by the coordinating atoms (E_1–E_4) (E = NH, O or S) were synthesized to systematically examine the electronic coupling effects between the two [Mo_2] units (Table 1, entry 2–4 and 8–10) [30–32]. Complexes with longer bridging ligands ($n = 2$) were synthesized (Table 1, entry 5–7) to study the distance dependence of electronic coupling and intramolecular electron transfer [33]. While most of the work was focused on bridging-ligand mediated metal–metal interaction, the substituent effects of the ancillary ligands on the electronic coupling were also investigated. A series of complexes with various *para*-substitutents R on the aryl rings have been designed and prepared (Table 1, entry 11–15) [34]. It is noteworthy that among all the 15 compounds listed, most of them have a symmetric bridging ligand ($E_1 = E_3$, $E_2 = E_4$). The only exception is compound **[O_2-(ph)$_1$-S_2]** (Table 1, entry 4), the bridging ligand of which contains a carboxylate group at one end and a dithiocarboxylate group at the other end. The study of this complex shed some light on the electronic communication in asymmetrical D–B–A complexes.

3. Development of synthetic procedure for the *dimers of dimers*

Dicarboxylate linked dimolybdenum and ditungsten dimers were first prepared in Chisholm's group by ligand substitution of the dimetal tetrakiscarboxylate with the corresponding acid [20–22], as shown in Eq. (1). Carboxylates with bulky alkyl groups, such as *t*-$BuCO_2^-$, are generally chosen as the ancillary ligands to increase the solubility of the starting materials. Toluene is a preferred solvent for the reaction, which allows the oligomeric product to be precipitated. However, reactions as such are divergent in nature, which may yield polymeric materials that compete with the target compounds.

$$2M_2(O_2CR)_4 + HO_2CR'CO_2H \longrightarrow [M_2(O_2CR)_3]_2(\mu\text{-}O_2CR'CO_2) + 2RCO_2H \quad M = Mo, W \tag{1}$$

Convergent syntheses of dimolybdenum dimers were achieved in Cotton's group in 1998. Two compounds, $[Mo_2(DAniF)_3]_2(\mu\text{-}O_2CCO_2)$ and $[Mo_2(DAniF)_3]_2(\mu\text{-}O_2CC_6F_4CO_2)$, were prepared by reaction of an oxidized precursor $Mo_2(DAniF)_3Cl_2$ with the dicarboxylate in the presence of reducing agent (Eq. (2)) and their structures were determined by single crystal X-ray diffraction [23].

$$2Mo_2(DAniF)_3Cl_2 + 2NaHBEt_3 + ({}^nBu_4N)_2(O_2CXCO_2) \longrightarrow [Mo_2(DAniF)_3]_2(\mu\text{-}O_2CXCO_2) + 2NaCl + 2({}^nBu_4N)Cl + 2BEt_3 + H_2 \tag{2}$$

For the oxalate analogue, *X* = nothing in Eq. (2). Compared to carboxylate, formamidinate is a better ancillary ligand to block the extra coordination sites due to its stronger Lewis basicity, which ensures the reaction proceeding toward the target compound. This procedure was further developed by using Zn dust as the reducing reagent and acetonitrile as solvent. The exciting achievement was the isolation of the acetonitrile coordinated intermediate $[Mo_2(DAniF)_3(NCCH_3)_2]^+$; on this basis, this synthetic method was standardized as shown in Eq. 3.

$$2Mo_2(DAniF)_3Cl_2 + Zn + 4MeCN \longrightarrow 2[Mo_2(DAniF)_3(MeCN)_2]^+ + ZnCl_4^{2-} \tag{3a}$$

$$2[Mo_2(DAniF)_3(MeCN)_2]^+ + ({}^nBu_4N)_2(O_2CXCO_2) \longrightarrow [Mo_2(DAniF)_3]_2(\mu\text{-}O_2CXCO_2) + 2({}^nBu_4N)^+ \tag{3b}$$

Using this procedure, a variety of dicarboxylate bridged dimolybdenum dimers were synthesized [24,35].

However, there exist some synthetic disadvantages in employing the oxidized precursor for preparing the *dimers of dimers*. Preparation of the dichloro complex $Mo_2(DAniF)_3Cl_2$ from $Mo_2(DAniF)_4$ takes about one week and a large amount of solvent (THF), and ends with a low yield. More importantly, its application is limited to assembling the dimolybdenum units with dicarboxylate bridging ligand. More basic ligands such as diamidate are not suitable for this method because the deprotonated bridging ligand would initiate a nucleophilic attack to the coordinated acetonitrile molecules, which give undesirable materials. This recognition was obtained after many efforts were made to synthesize the diamidate bridged analogues by following a similar approach [36]. The desired *dimers of dimers* with *N,N′*-diarylterephthaloyldiamidate (aryl = Ph or *m*-CF_3Ph) bridging ligands were eventually obtained in a modified procedure, in which $Mo_2(DAniF)_3Cl_2$ and the neutral diamide were mixed in THF and an excess amount of sodium alkoxide was added. The isolation of the alkoxyzincate-bridged dimolybdenum pairs $[Mo_2(DAniF)_3]_2[Zn(OR)_4]$ as an intermediate indicated that the acetonitrile derivative $[Mo_2(DAniF)_3(NCCH_3)_2]^+$ was not the immediate precursor for the assembling reaction [37]. This led to the designed synthesis of the building block material $Mo_2(DAniF)_3(O_2CCH_3)$, as shown in Eq. (4) and Fig. 3A. With this starting material, a convergent and more generalized method for assembling two dimolybdenum units with a diverse group of bridging ligands was developed (Eq. 5) [37].

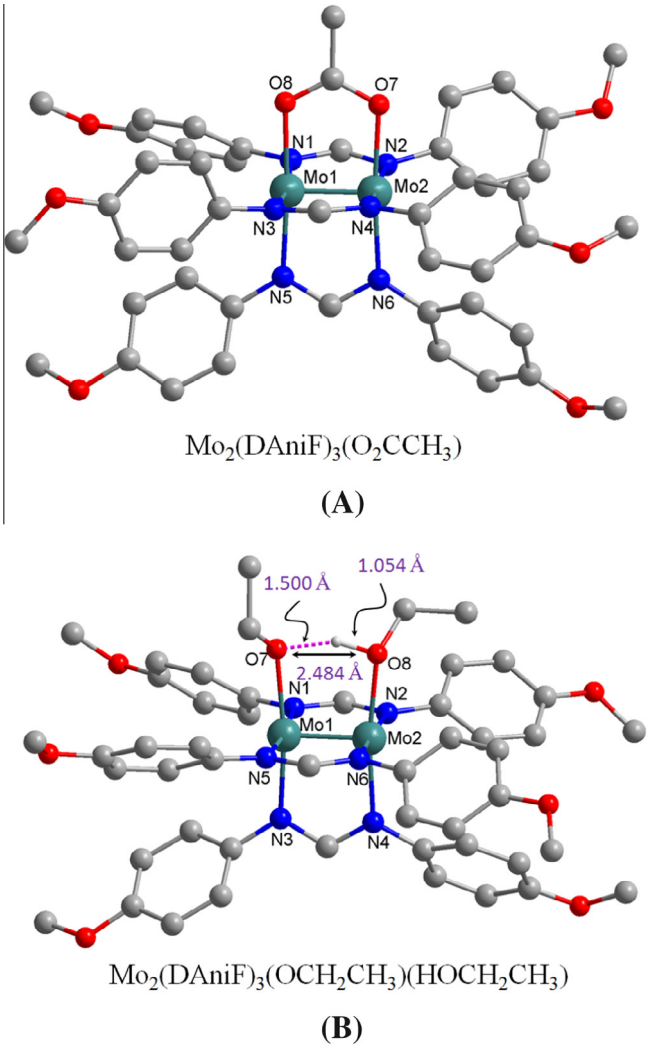

Fig. 3. X-ray crystal structures for $Mo_2(DAniF)_3(O_2CCH_3)$ (A) and $Mo_2(DAniF)_3(OCH_2CH_3)(HOCH_2CH_3)$ (B). The hydrogen atoms have been omitted, except for the hydroxyl group on the ethanol molecule.

$$Mo_2(O_2CCH_3)_4 + 3HDAniF + 3NaOCH_2CH_3 \longrightarrow Mo_2(DAniF)_3(O_2CCH_3) + 3NaO_2CCH_3 + 3CH_3CH_2OH \quad (4)$$

$$Mo_2(DAniF)_3(O_2CCH_3) + NaOCH_2CH_3 \longrightarrow Mo_2(DAniF)_3(OCH_2CH_3)(HOCH_2CH_3) + CH_3CO_2Na \quad (5a)$$

$$2Mo_2(DAniF)_3(OCH_2CH_3)(HOCH_2CH_3) + RHNOCXCONHR \longrightarrow [Mo_2(DAniF)_3]_2(\mu\text{-}RNOCXCONR) + 4CH_3CH_2OH \quad (5b)$$

Importantly, compound $Mo_2(DAniF)_3(O_2CCH_3)$ can be conveniently obtained by a one-pot reaction in good yield and purity [38]. The acetate on the molecule can be readily removed by addition of stoichiometric amount of sodium ethoxide in ethanol, generating the intermediate species, $Mo_2(DAniF)_3(OCH_2CH_3)(HOCH_2CH_3)$, which is isolated and structurally characterized. As shown in Fig. 3B, the $CH_3CH_2O^-$ anion and CH_3CH_2OH molecule in the structure are tied together by hydrogen bond and fill into a pair of equatorial coordination sites of the Mo_2 unit like a three-atom bridging ligand. In the assembling reaction with a bridging ligand, the coordinated ethoxide functions as 1 equiv. of base for deprotonation of the bridging ligand and the kinetically labile ethanol molecules are easily substituted by the incoming bridging ligand. Thus, this mixed-ligand complex $Mo_2(DAniF)_3(O_2CCH_3)$ can serve as an excellent starting material for the construction of the *dimers of dimers*. Since this method was developed, the synthesis of dimolybdenum dimers becomes more enjoyable bench work and a variety of the analogues, including those appearing in this article, have been synthesized using similar method [30–34,39–41].

4. Electrochemical study

For moderately strong coupling systems, the complexes exhibit two successive one electron redox processes for the two quadruply bonded Mo_2 centers. The magnitude of the potential separation ($\Delta E_{1/2}$) corresponds to the free energy change of the comproportionation reaction (ΔG_c), which therefore measures the thermodynamic stability of the mixed-valence species. It is recognized that there are several factors that influence the magnitude of ΔG_c, i.e., ΔG_s (statistical), ΔG_i (inductive), ΔG_e (electrostatic), and ΔG_r (resonance) [42]. Of the four terms, only the last two contribute to enhance the electronic communication. Therefore, the magnitude of $\Delta E_{1/2}$ can be utilized to weigh the strength of electronic communication only under certain circumstance, in which the differences for the first two factors are negligible.

Compounds in $(ph)_1$ series have very similar molecular and electronic structures. Variation of the donor atoms brings little change to the $Mo_2\cdots Mo_2$ nonbonding separation. Therefore, the difference in $\Delta E_{1/2}$ values is mainly due to the change of donor atoms; thus, the electrochemical data are comparable in concerning the metal–metal interaction. It is confirmed, through several molecular systems [41,44,45], that substitution of sulfur atoms for oxygen donor atoms on the bridging ligand significantly enhance the electronic interaction. This is further manifested by electrochemical measurements for the three compounds in a series, **[O$_2$-(ph)$_1$-O$_2$]**, **[OS-(ph)$_1$-OS]** and **[S$_2$-(ph)$_1$-S$_2$]** (Table 2) [30]. In this series, the $\Delta E_{1/2}$ values increase stepwise from 100 mV to 116 mV then to 195 mV. In contrast, the effect of changing the oxygen to nitrogen donors was not quite clear, although some diamidate bridged analogues were studied [36]. There could be two reasons for this. Firstly, the difference between N and O in modulating electronic coupling is very small; secondly, for N-substituted diamidate analogues, the electronic property of the substituents may significantly affect the metal–metal interaction. This puzzle was solved recently by the study on full-N donor analogue **[N$_2$-(ph)$_1$-N$_2$]**, which has a $\Delta E_{1/2}$ value of 80 mV, smaller than that for **[NO-(ph)$_1$-NO]** (96 mV) [32]. Both of the two N-containing molecules exhibit $\Delta E_{1/2}$ values smaller than that for **[O$_2$-(ph)$_1$-O$_2$]** (100 mV). For the S-donor derivative **[NS-(ph)$_1$-NS]**, the $\Delta E_{1/2}$ value is further increased to 115 mV. These results demonstrate that among the three types of donor atoms (N, O and S) we have so far investigated, the electronic effects for enhancing the electronic communication in the Mo_2–Mo_2 systems are in the order of S > O > N.

Interestingly, the *para*-substituents on the phenyl formamidinate ligands, located about 8 Å away from the Mo_2 center, affect the magnitude of $\Delta E_{1/2}$ as well. As the substituents vary from electron-donating to electron-withdrawing groups, the potential separations decrease accordingly [34]. For the series, the largest potential separation ($\Delta E_{1/2}$ = 86 mV in THF) is found for **[O$_2$-(ph)$_1$-O$_2$]** with the most electron-donating OCH_3 substituents, while **[O$_2$-(ph)$_1$-O$_2$]-CF$_3$** gives the smallest $\Delta E_{1/2}$ value of 49 mV. It is remarkable that the substituent effects on the electronic coupling can be best described by a linear correlation of the $\Delta E_{1/2}$ values versus the Hammett constants (σ_X). These results conform to the general principle that electron-donating substituents lower the redox potentials, while electron-withdrawing groups raise the potential values. The study also shows that changing the peripheral groups on the dimetal units may fine tune the donor-acceptor electronic coupling.

The unsymmetrical complex **[O$_2$-(ph)$_1$-S$_2$]**, however, has a notably large $\Delta E_{1/2}$ value, ca. 360 mV [30]. This is due to the presence of an intrinsic potential difference (ΔE_{ip}) between the two distinct redox centers. Hence, the magnitude of $\Delta E_{1/2}$ cannot be directly used to evaluate the metal to metal coupling interaction. To estimate the degree of electronic communication for **[O$_2$-(ph)$_1$-S$_2$]**, two monomers $Mo_2(DAniF)_3(O_2CC_6H_5)$ and $Mo_2(DAniF)_3(S_2CC_6H_5)$ that structurally and electronically resemble the two distinct $[Mo_2]$ units were exploited, which presumably have the half-wave potentials similar to those for the associated dimolybdenum centers. The potentials of oxidation $Mo_2^{4+} \rightarrow Mo_2^{5+}$ are measured to be 375 mV (versus Ag/AgCl) for $Mo_2(DAniF)_3(O_2CC_6H_5)$ and 651 mV (versus Ag/AgCl) for $Mo_2(DAniF)_3(S_2CC_6H_5)$. The potential difference of 276 mV is then taken as the internal potential difference (ΔE_{ip}) for **[O$_2$-(ph)$_1$-S$_2$]** and the "net" potential displacement is then

Table 2
Electrochemical, spectroscopic and ^{1}H NMR data for the complexes.

Compd.	$\Delta E_{1/2}$ (mV)[b]	λ_{max} (nm)	$\Delta\delta$ (ppm)[c]
[O$_2$-(ph)$_1$-O$_2$]	100	492	0.141
[OS-(ph)$_1$-OS]	116	618	0.178
[S$_2$-(ph)$_1$-S$_2$]	195	715	0.195
[O$_2$-(ph)$_1$-S$_2$]	360	637	0.151 (O_2) 0.203 (S_2)
[O$_2$-(ph)$_2$-O$_2$]	N/A	476	0.103
[OS-(ph)$_2$-OS]	N/A	577	0.146
[S$_2$-(ph)$_2$-S$_2$]	N/A	639	0.178
[N$_2$-(ph)$_1$-N$_2$]	80	465	0.192
[NO-(ph)$_1$-NO]	96	490	0.148
[NS-(ph)$_1$-NS]	115	560	0.125
[O$_2$-(ph)$_1$-O$_2$]-OCH$_3$[a]	86	491	0.141
[O$_2$-(ph)$_1$-O$_2$]-CH$_3$[a]	81	486	0.119
[O$_2$-(ph)$_1$-O$_2$]-F[a]	66	477	0.091
[O$_2$-(ph)$_1$-O$_2$]-Cl[a]	60	470	0.085
[O$_2$-(ph)$_1$-O$_2$]-OCF$_3$[a]	55	466	0.049
[O$_2$-(ph)$_1$-O$_2$]-CF$_3$[a]	49	457	0.240 (DMSO)

[a] For the *para*-substituted compounds **[O$_2$-(ph)$_1$-O$_2$]**-R, the electrochemical and spectroscopic measurements were performed in THF.

[b] The potential separation values ($\Delta E_{1/2}$) were obtained through differential pulse voltammogram (DPV) in 0.10 M CH_2Cl_2 or THF solution of $^nBu_4NPF_6$ using Richardson-Taube methods [43].

[c] $\Delta\delta = \delta_{\parallel} - \delta_{\perp}$ and the listed values were obtained in $CDCl_3$ unless otherwise noted.

determined to be 84 mV, reasonably less than that for [**O_2-(ph)$_1$-O_2**] (100 mV).

In $(ph)_2$ series, the $Mo_2\cdots Mo_2$ separation is increased to about 16 Å and the coupling is much weaker in comparison with that for the $(ph)_1$ series [33]. In the electrochemical process, the two one-electron oxidations occurring at the Mo_2^{4+} centers are not resolved. Electrochemical measurement is inapplicable for evaluation of the electronic coupling in this case.

5. Electronic absorption spectra and DFT calculation

For the *dimers of dimers* with conjugated bridges, the d(δ)–p(π) orbital interactions between the dimetal units and bridging ligand can be qualitatively described by Fig. 4. This simplified frontier MO diagram is very helpful in understanding the metal-ligand and the metal–metal interactions. The HOMO results from the out-of-phase ($\delta - \delta$) combination of the δ orbitals with a filled π orbital of the bridging ligand, while the HOMO-1 is obtained by the in-phase ($\delta + \delta$) combination of the δ orbitals with an empty π^* orbital from the ligand. These two occupied metal based orbitals are non-degenerate because of the metal-ligand interactions. While the HOMO–LUMO energy gap (ΔE_{H-L}) predicts the metal to ligand transition energy, the energy difference between HOMO and HOMO-1, or ΔE_{H-H-1}, signals the strength of the electronic interaction between the two [Mo_2] units. Small ΔE_{H-L} value indicates a low energy for metal to ligand charge transfer, which enhances the metal–metal coupling. On the other hand, the stronger the metal–metal interaction becomes, the larger the magnitude of ΔE_{H-H-1} is. It is clear that in such a system, only the δ electrons are involved in the metal to ligand as well as the metal–metal interactions. There is no doubt that the well defined electronic structure for the *dimers of dimers* is greatly beneficial to the study of metal–metal coupling interaction.

In the spectra, the complexes display an intense absorption band in visible region. The observed transition energies are generally in good agreement with the ΔE_{H-L} values calculated at the DFT level [30]. Therefore, these bands are assigned to the HOMO → -LUMO excitation, or metal to ligand charge transfer (MLCT). For both $(ph)_1$ and $(ph)_2$ series, the band energy decreases but the intensity increases as the donor atoms change from O to S. In $(ph)_1$ series, replacements of the first and second two oxygen atoms by sulfur lower the MLCT energy by 145 and 223 nm, respectively [30], while the corresponding energy changes are 101 and 163 nm for $(ph)_2$ series [33] (Table 2). As expected, the ML transition occurs at a relatively high energy region for the $(ph)_2$ series. However, for the tetrathiolated analogues, the blue shifts of the MLCT band are larger than those for dicarboxylate and dithiocarboxylate systems. It is interesting to note that the two dithiolated complexes, [**OS-(ph)$_1$-OS**] and [**O_2-(ph)$_1$-S_2**], display the MLCT bands with similar band energies and intensities, i.e. 637 nm (ε, $2.6 \times 10^4\ M^{-1}\ cm^{-1}$) for the latter and 618 nm (ε, $2.3 \times 10^4\ M^{-1}\ cm^{-1}$) for the former [30]. For the analogues with N and O donor atoms, similar absorption energies and intensities are observed. The MLCT for [**N_2-(ph)$_1$-N_2**] appears at 465 nm, while slightly lower band energy (492 nm) was observed for [**O_2-(ph)$_1$-O_2**] (Table 2) [32]. In N-donor containing series, substitution of two N donor atoms with O atoms shifts the MLCT band from 465 nm ([**N_2-(ph)$_1$-N_2**]) to 490 nm ([**NO-(ph)$_1$-NO**]), and with S atoms the band wavelength further shifts to 560 nm ([**NS-(ph)$_1$-NS**]). Hence, the electronic spectra and DFT calculations confirm that the enhancement of the electronic interaction by the coordinating atoms follows the sequence of S > O > N.

As shown in Table 2, substituents on the [Mo_2] units also have significant influence on the ML transition energy.[34] In the series with terephthalate bridging ligand but varying ancillary ligands for the Mo_2 units, strong electron-donating ability of the methoxy groups (OCH_3) renders [**O_2-(ph)$_1$-O_2**] the lowest electronic transition energy, while the compound with strong electron-withdrawing groups, [**O_2-(ph)$_1$-O_2]-CF_3**, displays an absorption band having the highest energy. For [**O_2-(ph)$_1$-O_2**], the low energy MLCT band suggests a small HOMO–LUMO energy gap (ΔE_{H-L}). Obviously, the electron-donating groups, e.g., OCH_3, are capable of raising the energy level of the δ orbitals, which lowers the ΔE_{H-L} energy gap. In contrary, the electron-withdrawing property of the CF_3 substituents on [**O_2-(ph)$_1$-O_2]-CF_3** should be responsible for its high energy MLCT band and large ΔE_{H-L} value. It is remarkable that for the *para*-substituted series, the charge transfer energies (λ_{max}) are correlated to the Hammett constants of the substitutents (σ_x) by a linear relationship with $R^2 = 0.998$, $\lambda_{max} = 1771\text{-}\sigma_x + 20859$, as shown in Fig. 5. Therefore, these results indicate that fine-tuning the ML transition can be realized by varying the remote peripheral groups on the redox centers.

6. ^{1}H NMR Spectra

Additional advantage of employing formamidinate supporting ligands for the dimolybdenum dimers is that the NMR chemical shifts of the methine protons reflect the electron density on the charge transfer platform involving the two [Mo_2] units and bridging ligand. The methine protons on the vertical ($H_\perp$) and horizontal ($H_\parallel$) formamidinate ligands resonate at different chemical shifts, $\delta_\perp$ and $\delta_\parallel$, respectively, as shown in Fig. 6. It is found that the displace-

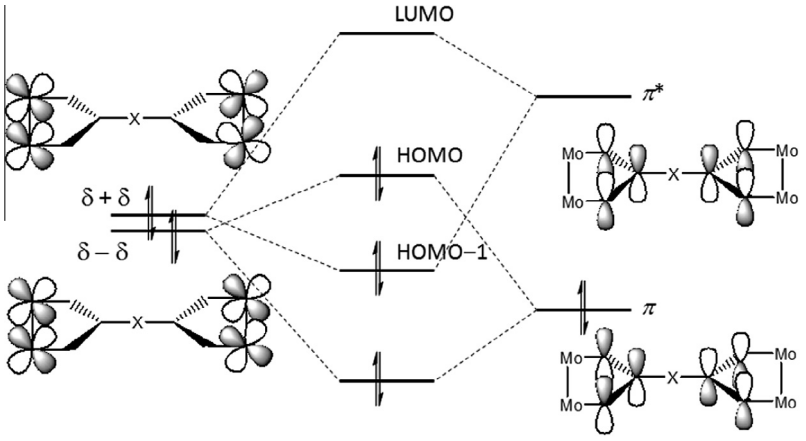

Fig. 4. A qualitative molecular orbital diagram showing the orbital interactions between the dimetal units (d_δ) and the bridging ligand (p_π).

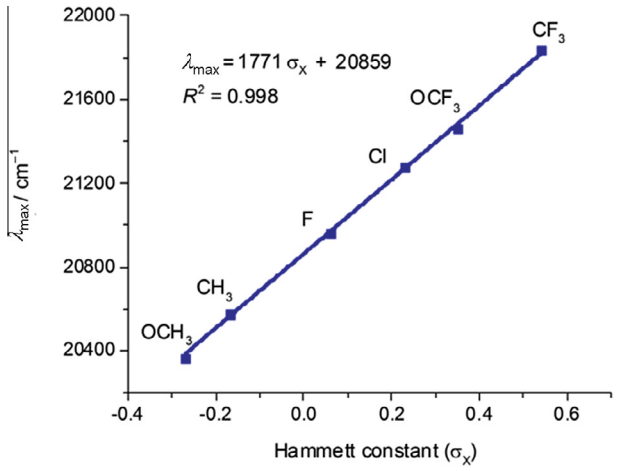

Fig. 5. A plot of metal to ligand transition energy (λ_{max}) vs. the Hammett constant (σ_x) of the *para*-substituents on the peripheral ligands. Linear fitting gives a correlation coefficient (R^2) of 0.998.

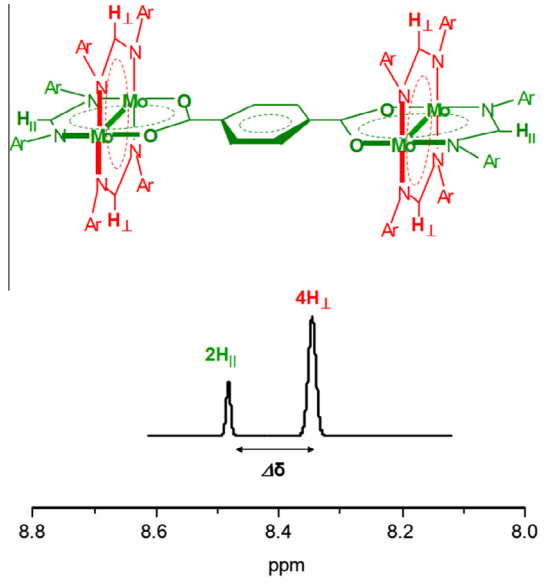

Fig. 6. Schematics of aryl formamidinate supported dimolybdenum dimer accompanied with the selective ^{1}H NMR spectrum for the methine protons in two orthogonal positions ($H_{||}$ and $H_\perp$).

ment between $\delta_\perp$ and $\delta_{||}$, i.e., $\Delta\delta = \delta_{||} - \delta_\perp$, is correlated to the extent of electron delocalization over the two [Mo_2] sites. As shown in Table 2, for complexes with O and S donor atoms on the bridging ligands, the separation for $\delta_\perp$ and $\delta_{||}$ increases as the electronic interaction increases. The variation tendency of $\Delta\delta$ is parallel to those for electrochemical ($\Delta E_{1/2}$) and spectroscopic (λ_{max}) parameters. Particularly, by varying substituents on the ancillary ligands, a linear correlation of $\Delta\delta$ with the Hammett constants (σ_X) is observed [34]. Interestingly, for those having N donors on the bridging ligands, the variation tendency of $\Delta\delta$ is reversed, which is not well understood yet. Nevertheless, this diamagnetic parameter provides a unique probe for charge delocalization in the [Mo_2]–bridge–[Mo_2] systems and can be used to evaluate the strength of the electronic interaction between the two [Mo_2] units.

7. General mixed-valence properties for the singly oxidized complexes

The MV cation radicals were prepared by one-electron oxidation of the corresponding neutral molecules using one equiv. of ferrocenium hexafluorophosphate (Cp_2FePF_6) in CH_2Cl_2 solution and characterized by EPR spectra. For the complexes presented in Table 3, the *g* values of 1.940–1.948 are significantly smaller than that for a free organic radical (ca. 2.0023). This suggests that the unpaired electron resides mainly on a Mo-based orbital. Similar *g* values for the series of MV compounds indicate that the complexes have similar electronic structures. Notably, as shown in Table 3, for the three series presented, the *g* values increase as the electronic coupling is enhanced by introduction of S donor atoms, although the variation is small.

The most striking spectroscopic feature for the MV complexes is the weak and broad absorption band in near-IR to mid-IR region, which should be assigned to intervalence (IV) or metal to metal (MM) charger transfer. In general, the singly oxidized compounds show the MLCT band with transition energy similar to that for the neutral molecule but lower intensity as shown in Figs. 7 and 8. This is a reflection that the MV compounds are in the Class II or valence trapped regime. In addition to the MLCT and IV bands, some MV complexes present a ligand to metal charge transfer (LMCT) band. Presumably, the energy level of the δ orbital for the singly oxidized [Mo_2] unit (the acceptor) is lower than that for the neutral [Mo_2] unit (the donor); therefore, the energy gap between the metal and ligand orbitals on the acceptor site is smaller than that on the donor site. This is confirmed by the observation that the LMCT band shows as a shoulder at low energy side of the MLCT band (Fig. 7). It is also worthwhile to note that the MV complexes with sulfur donors on the bridging ligand usually present a LMCT and the intensity increases as the number of sulfur atoms increase. Importantly, compared to other mixed-valence systems, such as dinuclear d^5-^{6} and Ru_3–Ru_3 complexes as well as organic D–B–A compounds, the *dimers of dimers* exhibit "clear and clean" absorption bands that are related to the intervalence transition. These features largely facilitate the analysis for electronic coupling and electron transfer. It is also noteworthy that in the [Mo_2]–bridge–[Mo_2] system, subtle difference of the bridging ligands result in significant variation to the energy, intensity and shape of the IV bands as shown in Table 4.

In the N-containing series, changing the donor atoms of the bridging ligand from N to O to S gradually lowers the IV transition energies and increases the absorption intensities (Fig. 8) [32]. For example, the IV band for amidinate bridged complex **[N_2-(ph)$_1$-N_2]$^+$** appears at 4980 cm^{-1}. This band is slightly red shifted to 4651 cm^{-1} for the amidate analogue **[NO-(ph)$_1$-NO]$^+$**, and further down to 3182 cm^{-1} for the thioamidate derivative **[NS-(ph)$_1$-NS]$^+$**. For both (ph)$_1$ and (ph)$_2$ series, the complexes with the lowest IV band energy and highest intensity are those with fully thiolated bridging ligands, **[S_2-(ph)$_1$-S_2]$^+$** and **[S_2-(ph)$_2$-S_2]$^+$**. As expected, for the two dithiolated species, **[OS-(ph)$_1$-OS]$^+$** and **[O_2-(ph)$_1$-S_2]$^+$**, the asymmetrical complex has the IV band energy higher than that for

Table 3
g values of EPR spectra for the cation radicals.[a]

Compd.	**[O_2-(ph)$_1$-O_2]$^+$**	**[OS-(ph)$_1$-OS]$^+$**	**[S_2-(ph)$_1$-S_2]$^+$**	**[O_2-(ph)$_1$-S_2]$^+$**
g	1.942	1.945	1.947	1.943
Compd.	**[O_2-(ph)$_2$-O_2]$^+$**	**[OS-(ph)$_2$-OS]$^+$**	**[S_2-(ph)$_2$-S_2]$^+$**	
g	1.944	1.945	1.946	
Compd.	**[N_2-(ph)$_1$-N_2]$^+$**	**[NO-(ph)$_1$-NO]$^+$**	**[NS-(ph)$_1$-NS]$^+$**	
g	1.940	1.946	1.948	

[a] Samples were measured *in situ* in CH_2Cl_2 at 110 K.

the symmetrical one due to the intrinsic potential difference between the donor and acceptor [31]. This optical behavior is consistent with the electrochemical property as discussed above. For $(ph)_2$ series, there are two factors, i.e., the long donor-acceptor separation (ca. 15 ~ 16 Å) and the torsion angle (ca. 30°–50°) between the two phenyl rings, that increase the IV band energies and lower the intensities, thus, diminishing the electronic coupling [33].

In terms of the extent of electron delocalization, the broadness of MMCT absorption bands for MV complexes can be measured by comparing the experimental bandwidth ($\Delta\nu_{1/2}$) with the calculated value ($\Delta\nu^{o}_{1/2} = (2310E_{IT})^{1/2}$). According to the equation derived from the Hush model, $\Gamma = 1 - \Delta\nu_{1/2}/(2310E_{IT})^{1/2}$ [46], a broader IV band gives rise to a small Γ value (<0.5), meaning that the donor and acceptor sites are weakly coupled. In these dimolybdenum systems, the IV bands are generally broader in shape and lower in energy than those for the bridged dinuclear d^{5-6} complexes. For some species discussed, negative Γ values are found (Table 4), indicating that the mixed-valence series belong to the weakly coupled Class II regime. As expected, the Γ value increases in order as the sulfur atoms are stepwise introduced into the bridging ligand (Table 4) [30]. Among the listed complexes, the fully thiolated $[\mathbf{S_2}\text{-}(\mathbf{ph})_\mathbf{1}\text{-}\mathbf{S_2}]^+$ ($\Gamma = 0.30$) is on the Class II-III borderline as judged from the appreciable "cut off" of the IV band (Fig. 7C). The variation of broadness of the IV bands (or the Γ values) shows that by changing the donor atoms and the bridge length, the donor-acceptor interactions vary from weakly to moderately strongly coupled until reaching the Class II-III borderline.

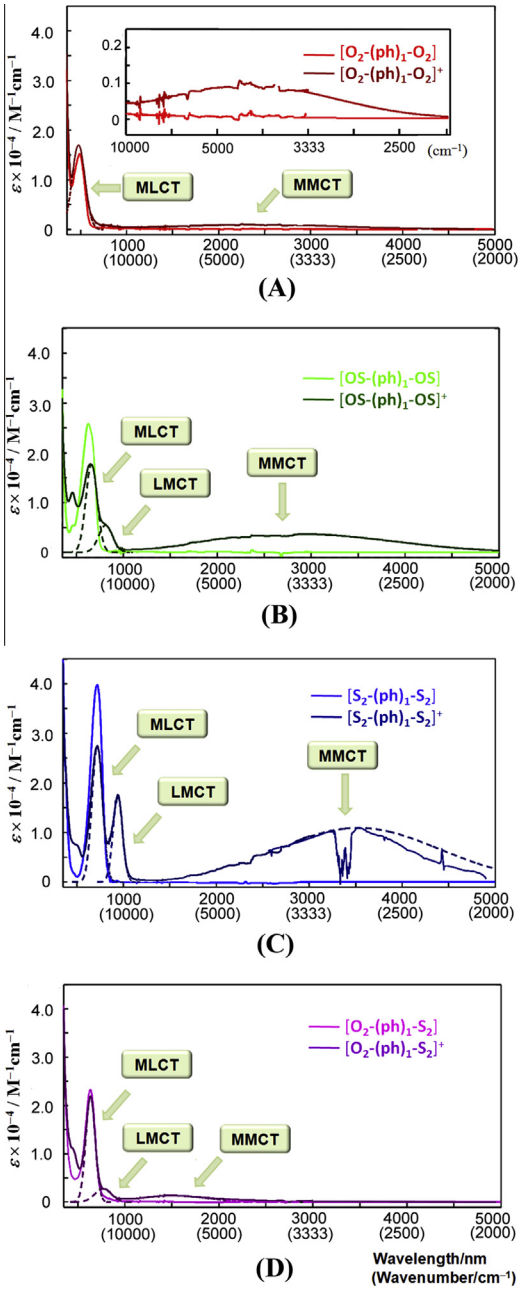

Fig. 7. Comparison of Vis-Near-IR-Mid-IR spectra (measured in CH_2Cl_2) of the neutral and the mixed-valence complexes differentiated by donor atoms O and S in $(ph)_1$ series.

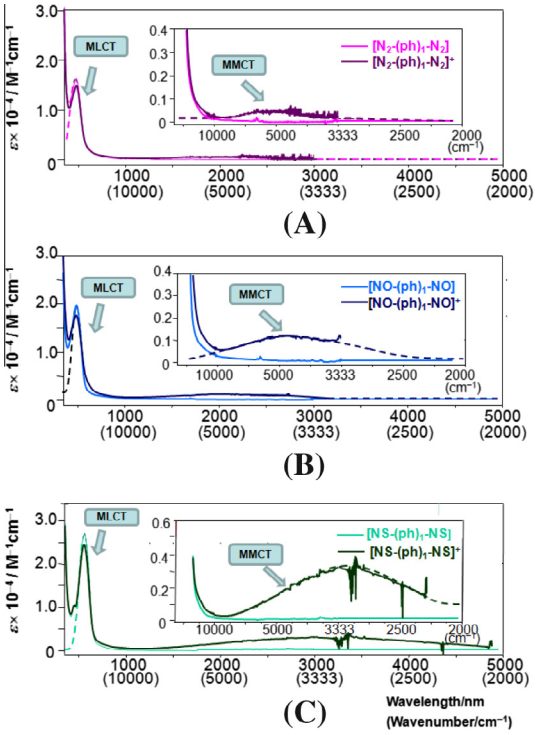

Fig. 8. Comparison of the Vis-Near-IR-Mid-IR spectra for the neutral and the mixed-valence complexes differentiated by donor atoms N, O and S in the N-containing series.

8. Electronic coupling elements calculated from the Hush model

The electronic coupling matrix element for a mixed-valence D–B–A system can be derived from the widely accepted Mulliken-Hush expression (Eq. (6)) [47,48], which successfully correlates the IVCT band parameters with the thermal ET energy barrier or activation energy ΔG^* in the Marcus theory [49,50].

$$H_{ab} = 2.06 \times 10^{-2} \frac{(\Delta\nu_{1/2}\varepsilon_{max}E_{IT})^{1/2}}{r_{ab}} \quad (6)$$

In this equation, r_{ab} is the electron transfer distance, which is usually determined from the geometrical separation between the two metal centers. However, as pointed out in the literature [51,52], adopting metal to metal distance for r_{ab} would lead to an underestimated H_{ab} value because the actual electron transfer distance (r'_{ab}) is significantly shorter [53,54]. When applicable, r'_{ab} can be obtained from the dipole moment change in Stark effect [55,56]. For the covalently bonded dimetal systems, we seek for an experimental approach to estimate r'_{ab} for determination of

Table 4
Intervalence absorption bands of the mixed-valence complexes.[a]

Compd.	E_{IT} (cm^{-1})	ε_{IT} (M^{-1} cm^{-1})	$\Delta\nu_{1/2}$ (cm^{-1})	$\Delta\nu^{o}_{1/2}$ (cm^{-1})	Γ	H_{ab} (cm^{-1})	E_{ML}[b] (cm^{-1})	ε_{ML}[b] (M^{-1} cm^{-1})	E_{LM} (cm^{-1})	ε_{LM} (M^{-1} cm^{-1})	$H_{MM'}$ (cm^{-1})
[O_2-(ph)$_1$-O_2]$^+$	4240	1470	4410	3190	−0.17	589	20600	15230	0	0	551
[OS-(ph)$_1$-OS]$^+$	3440	3690	3290	2820	−0.14	727	16040	25870	12330	5445	764
[S_2-(ph)$_1$-S_2]$^+$	2640	12660	1770	2470	0.30	864	13850	39960	10630	17500	864
[O_2-(ph)$_1$-S_2]$^+$	6560	2270	4130	3890	−0.06	NA	15920	22500	12970	2780	711
[O_2-(ph)$_2$-O_2]$^+$	8300	198	8578	4379	−0.96	245	21012	9272	0	0	209
[OS-(ph)$_2$-OS]$^+$	6536	715	6338	3886	−0.63	354	17319	21840	0	0	294
[S_2-(ph)$_2$-S_2]$^+$	4826	1610	5231	3339	−0.56	415	15647	37350	0	0	348
[N_2-(ph)$_1$-N_2]$^+$	4980	520	8840	3392	−1.45	537	16310	5447	0	0	626
[NO-(ph)$_1$-NO]$^+$	4651	1171	5242	3278	−0.60	600	18370	4997	0	0	661
[NS-(ph)$_1$-NS]$^+$	3182	3589	3688	2711	−0.36	697	27140	3712	0	0	704

[a] r'_{ab} = 5.8 Å for phenylene bridged species and r'_{ab} = 10 Å for biphenylene bridged species.
[b] The E_{ML} and ε_{ML} data were measured from the neutral complexes.

H_{ab}. As is well known, the δ electrons on the dimetal center are delocalized over the coordination shell through d(δ)–p(π) conjugation, which apparently shortens the electron transfer distance [28,57]. In addition, the redox potential of a [Mo_2] unit is very sensitive to the equatorial ligands [58]. Since the D–B–A molecules are constructed by the same Mo_2 building blocks, the difference in electron-donating (or accepting) ability of the donor (or acceptor) between the analogues is due to the versatile chelating groups from the bridging ligands. Thus, the coordinatively saturated complex unit as a whole, rather than the $Mo_2^{4+/5+}$ cation, functions as the electron donor or acceptor. The central moiety "–C(C_6H_4)$_n$C–" that connects the electron donor and acceptor is considered to be the "real bridge" as shown in Fig. 9. Thereby, the effective ET distance (r'_{ab}) is reasonably estimated to be 5.8 Å for (ph)$_1$ series and 10 Å for (ph)$_2$ series. Given the spectroscopic data, calculations from Eq. (6) yielded the H_{ab} parameters for the complex series as listed in Table 4. The magnitudes of H_{ab} are generally comparable with those for MV complexes in other systems with similar metal–metal separations, for which the effective electron transfer distances r'_{ab} are estimated by Stark effect. For instance, with r'_{ab} = 5.8 Å, **[S_2-(ph)$_1$-S_2]$^+$** has a H_{ab} value of 864 cm^{-1}, close to the reported value for [{(NH_3)$_5$Ru}$_2$(μ-4,4′-bpy)]$^{5+}$ (900 cm^{-1}) [55].

9. Electronic coupling elements calculated from superexchange formalism

Based on the McConnell's superexchange theory [58], Creutz, Newton and Sutin proposed an alternative approach to calculate the electronic coupling matrix element (H'_{MM}, to distinguish from H_{ab}) [59]. By the CNS formalism, the calculation of H'_{MM} involves three equations (Eqs. (7)–(9)).

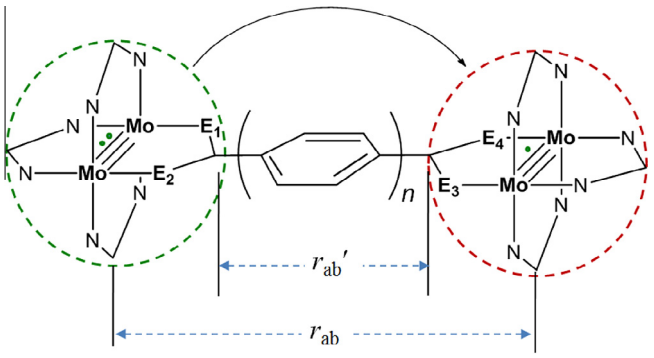

Fig. 9. Estimation of the effective electron transfer distance (r'_{ab}) in {[Mo_2]–bridge–[Mo_2]}$^+$.

$$H_{MM'} = \frac{H_{ML}H_{M'L}}{2\Delta E_{ML}} + \frac{H_{LM}H_{LM'}}{2\Delta E_{LM}} \quad (7)$$

$$\frac{1}{\Delta E_{ML}} = 0.5 \times \left(\frac{1}{E_{ML} - E_{IT}} + \frac{1}{E_{ML}}\right) \quad (8)$$

$$\frac{1}{\Delta E_{LM}} = 0.5 \times \left(\frac{1}{E_{LM} - E_{IT}} + \frac{1}{E_{LM}}\right) \quad (9)$$

According to Eq. (7), electronic coupling constant H'_{MM} is composed of two components, i.e. the contributions from metal to ligand (the first term) and ligand to metal charge transfer (the second term). These two terms correspond to the electron-hopping and hole-hopping pathway, respectively, which act synergistically in the course of electron transfer. Eq. (8) and (9) are given to calculate the effective energy gaps for metal to ligand (ΔE_{ML}) and ligand to metal (ΔE_{ML}) charge transfer from the optical data. By employing the Mulliken-Hush expression (Eq. (6)), the metal-ligand electronic coupling constant (H_{ML}) is derived from the MLCT absorption of the neutral precursor, while the ligand-metal coupling parameter (H_{LM}) is calculated from the LMCT band of the mixed-valence complex, if applicable [60]. However, not all the intramolecular electron transfer processes involve both pathways. Single pathway dominated systems, either by electron-hopping [60,61] or hole-hopping [42], have been reported for several systems and the CNS equations are usually simplified accordingly. In the present Mo_2–Mo_2 systems, the sulfur donor atoms on the bridging ligands are capable of enhancing the MLCT, as reported elsewhere [41,44], and improving the LMCT as well. For the relatively weak coupling systems, for example, the terephthalate bridged analogue and those in (ph)$_2$ series, the LMCT is not resolved, in case of which the electron transfer is treated as electron-hopping pathway only [33]. The coupling constants of 626 cm^{-1} for **[N_2-(ph)$_1$-N_2]$^+$** and 661 cm^{-1} for **[NO-(ph)$_1$-NO]$^+$** indicate quantitatively that the electronic coupling increases as nitrogen donors are replaced by oxygen atoms, which is supported by the electrochemical and spectroscopic results [32].

Testing of the latest theoretical model on determination of electronic matrix elements has been carried out in binuclear ruthenium [42,60–62] and organic systems [63]. However, significant discrepancies were found in results obtained from the two distinct models. Remarkably, our results show that the magnitudes of H'_{MM} from the CNS equations are in excellent agreement with the H_{ab} values derived from the Hush model, with H_{ab}/H'_{MM} ratio around 1 as shown in Table 4. For **[S_2-(ph)$_1$-S_2]$^+$** and **[NS-(ph)$_1$-NS]$^+$**, the two spectral methods give almost the same values. For **[N_2-(ph)$_1$-N_2]$^+$** and **[NO-(ph)$_1$-NO]$^+$**, the small deviations of ±100 cm^{-1} are essentially within experimental errors. Such a good consistency has not been obtained in other systems since the CNS model was proposed [42,60–63]. For the unsymmetrical analogue **[O_2-(ph)$_1$-S_2]$^+$**, only

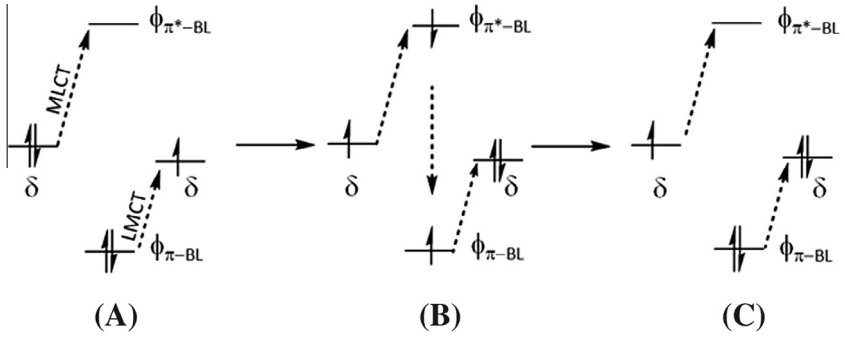

Fig. 10. Schematic illustration of superexchange mechanism for the electron transfer from the donor to the acceptor *via* the bridge. (A) Electron hopping from the δ orbital of the donor to the empty bridging π^* orbital; meanwhile, hole hopping from the δ orbital of the acceptor to the low-lying filled bridging π orbital. The MLCT and LMCT correspond to the electron and hole hopping, respectively. (B) A possible intermediate state of electron transfer at which the odd electrons on the ligand are paired in the bonding orbitals through relaxation. (C) Completion of electron transfer.

the CNS equations are applicable, which yielded a H'_{MM} value of 711 cm^{-1}, reasonably smaller than the value of 764 cm^{-1} for the symmetric isomer **[OS-(ph)$_1$-OS]$^+$** [31]. Obviously, application of effective electron transfer distance (r'_{ab}) for the Mulliken-Hush equation is important to achieve the conformity between the two approaches. On this basis, the latest superexchange approach is revalidated in the dimetal systems. These results demonstrate that the [Mo_2]–bridge–[Mo_2] systems are desirable D–B–A model compounds for experimental and theoretical studies in the field of electronic coupling and electron transfer.

As mentioned earlier, in superexchange framework, electron transfer from donor to acceptor crossing the bridge may proceed through two possible pathways, electron-hopping or hole-hopping. For the [Mo_2]–bridge–[Mo_2] systems studied, the two pathways occur simultaneously in some complexes, as indicated by the presence of both MLCT and LMCT bands [31], while in others, only electron-hopping takes place, thus, showing only the MLCT in the spectra [32,33]. Whether or not hole-hopping is involved in the ET process depends on the nature of the bridging ligand. According to the observed electronic spectra, shortening the bridge or introducing sulfur donor atoms promotes significant hole-hopping. By orbital description, the MLCT band is caused by an electron transition from $\delta(Mo_2)$ to empty $\phi_{\pi*-BL}$ of the bridge, while the LMCT is due to the electron transition from the filled $\phi_{\pi-BL}$ to the singly occupied δ orbital, or hole hopping in the reverse direction. From this point of view, the spectroscopic data and the derived coupling constants confirm that the electron transfer from donor to acceptor proceeds by electron hopping and hole hopping pathways, as described in Fig. 10. The excellent consistency for the electronic coupling parameters derived from the Hush model and the CNS formalism provide a straightforward interpretation of the effective two-state model.

Table 5
Calculated activation energies (ΔG^*) and ET rate constants (k_{et}).

Compd.		ΔG^* (cm^{-1})	k_{et} (s^{-1})
[O_2-(ph)$_1$-O_2]$^+$		581	3.0×10^{11}
[OS-(ph)$_1$-OS]$^+$		266	1.4×10^{12}
[S_2-(ph)$_1$-S_2]$^+$		79	3.4×10^{12}
[O_2-(ph)$_1$-S_2]$^+$	Forward	2430	3.4×10^{7}
	Reverse	364	8.6×10^{11}
[O_2-(ph)$_2$-O_2]$^+$		1838	7.0×10^{8}
[OS-(ph)$_2$-OS]$^+$		1299	9.5×10^{9}
[S_2-(ph)$_2$-S_2]$^+$		827	9.2×10^{10}
[N_2-(ph)$_1$-N_2]$^+$		766	1.2×10^{11}
[NO-(ph)$_1$-NO]$^+$		640	2.3×10^{11}
[NS-(ph)$_1$-NS]$^+$		251	1.5×10^{12}

10. Kinetics of the intramolecular transfer reaction

For weakly coupled systems (Class II), the kinetics of electron transfer reaction is discussed according to the semi-classical theories (Eqs. (10) and (11)) [55,64],

$$\Delta G^* = \frac{(\lambda - 2H_{ab})^2}{4\lambda} \tag{10}$$

$$k_{et} = A\exp(-\Delta G^*/k_B T) \tag{11}$$

where ΔG^* is the activation energy of the ET reaction and A is the pre-factor of the Arrhenius equation. For symmetrical Class II systems, the reorganization energy λ equals the vertical excitation energy E_{IT}. In the first-order adiabatic system (or Class II), the vibrational motion (10^{12}–10^{13} s^{-1}) is slower than the electronic motion (>>10^{14} s^{-1}). The pre-factor A is then determined by an averaged nuclear vibration frequency factor, that is, $\nu_n = 5 \times 10^{12}$ s^{-1}. Table 5 presents the calculated kinetic parameters for some [Mo_2]–bridge–[Mo_2] systems. The ET rate constants (k_{et}) for the symmetrical $(ph)_1$ series fall in the range of 10^{11}–10^{12} s^{-1}. The optically determined ET rates in the dimolybdenum systems are comparable with those observed in the Ru_3–Ru_3 systems [14,65], and those for organic D–B–A systems with conjugated bridges [66]. However, it is interesting to note that in our study, the ultrafast intramolecular electron transfer is observed in the systems in which the donor and acceptor sites are weakly or moderately strongly coupled ($2H_{ab} \ll \lambda$) [67]. The exceptionally fast ET must be attributed to the d(δ)–p(π) conjugation between the donor/acceptor and the bridge. Therefore, it is evident that orbital overlap is one of the major factors that govern the intramolecular electron transfer. For the three long-range weakly coupled complexes in $(ph)_2$ systems, the adiabatic electron transfer rate constants (k_{et}) fall in the range of 10^9–10^{11} s^{-1}, showing a distance dependence in comparison with the k_{et} data for $(ph)_1$ series [33]. These results are also compatible with mixed-valence systems having similar donor–acceptor separations [63,68]. For the unsymmetrical species, **[O_2-(ph)$_1$-S_2]$^+$**, the ground state has the S-coordinated [Mo_2] unit as the electron donor and O-coordinated [Mo_2] unit as the acceptor and the electron transfer reaction has a free energy change of 2250 cm^{-1} [30], being the case of $\Delta G^\circ > 0$ as shown in Scheme 1. The electron transfer from donor to acceptor occurs at $k_{et} = 3.4 \times 10^7$ s^{-1}. The rate constant for the reverse process is determined to be 8.6×10^{11} s^{-1}.

11. Concluding Remarks

The D–B–A complexes consisting of quadruply bonded [Mo_2] units as the electron donor (D) and acceptor (A) exhibit two

successive one-electron redox processes and single metal to ligand, ligand to metal and metal to metal charge transfer absorption bands in the electronic and vibronic spectra, which are exclusively due to the unique electronic structure of the Mo–Mo δ bonds. In the presented study, systematic variation of coordinating atoms (N, O or S), length of bridging ligands and electronic properties of ancillary ligands results in regulation of the electronic coupling between the two [Mo_2] sites. The electronic coupling matrix elements (H) for the systems are spectroscopically determined by employing the Hush vibronic model and the CNS superexchange formalism. According to the structural and electronic features of the [Mo_2] unit, the geometrical length of the "–C(C_6H_4)$_n$C–" spacer in the molecules were commonly taken as the effective electron transfer distance (r'_{ab}) in the Mulliken-Hush expression, which is critical for accurate determination of the H parameter. In application of the CNS equations, the two electron transfer pathways, i.e. electron-hopping and hole-hopping, are taken into account in some cases, while in other cases only electron-hopping pathway is considered for the electron transfer process. Remarkably, in both situations, the coupling constants derived from the two distinct theoretic frameworks are very consistent with each other, in sharp contrast to the notable discrepancy observed in other donor-acceptor systems. On this basis, the electron transfer kinetic parameters, activation energy (ΔG^*) and rate constant (k_{et}), are determined under the Marcus–Hush semi-classical theoretical framework. For the [Mo_2]–bridge–[Mo_2] systems investigated, the electron transfer rate constants are found in the range of 10^8–10^{12} s^{-1}, which are compatible with the data for other systems with similar donor-acceptor separation.

Therefore, the research described herein illustrates that the [Mo_2]–bridge–[Mo_2] systems are excellent model compounds for the study of electronic coupling and intramolecular electron transfer. This research effort is to open up new research areas, which are based upon Al Cotton's pioneering work half a century ago.

Acknowledgments

We thank the National Science Foundation of China (No. 20871093, 90922010, 21371074 and 21301070), Jinan University and Tongji University for financial support.

Appendix A. Supplementary material

Supplementary data associated with this article can be found, in the online version, at http://dx.doi.org/10.1016/j.ica.2014.09.039.

References

[1] A. Osyczka, C.C. Moser, F. Daldal, P.L. Dutton, Nature 247 (2004) 607.
[2] M.T. Tierney, M. Sylora, S.I. Khan, M.W. Grinstaff, J. Physf, Chem. B 104 (2000) 7574.
[3] T.F. Ho, A.R. McIntosh, J.R. Bolton, Nature 286 (1980) 254.
[4] Y.H. Huang, C.T. Rettner, D.J. Auerbach, A.M. Wodtke, Science 290 (2000) 111.
[5] H. Wang, S. Lin, J.P. Allen, J.C. Williams, S. Blankert, C. Laser, N.W. Woodbury, Science 346 (2007) 747.
[6] A. Kumar, M.D. Sevilla, Chem. Rev. 110 (2010) 7002.
[7] N.S. Hush, Coord. Chem. Rev. 64 (1985) 135.
[8] M.B. Robin, P. Day, Adv. Inorg. Chem. Radiochem. 10 (1967) 247.
[9] C. Creutz, H. Taube, J. Am. Chem. Soc. 91 (1969) 3988.
[10] C. Creutz, H. Taube, J. Am. Chem. Soc. 95 (1973) 1086.
[11] C. Creutz, Prog. Inorg. Chem. 30 (1983) 1.
[12] R.J. Crutchley, Adv. Inorg. Chem. 41 (1994) 273.
[13] D.E. Richardson, H. Taube, Coord. Chem. Rev. 60 (1984) 107.
[14] T. Ito, T. Hamaguchi, H. Nagino, T. Yamaguchi, J. Washington, C.P. Kubiak, Science 277 (1997) 660.
[15] J.C. Salsman, C.P. Kubiak, J. Am. Chem. Soc. 127 (2005) 2382.
[16] B.J. Lear, S.D. Glover, J.C. Salsman, C.H. Londergan, C.P. Kubiak, J. Am. Chem. Soc. 129 (2007) 12772.
[17] A.A. Bakulin, S.D. Dimitrov, A. Rao, P.C.Y. Chow, C.B. Nielsen, B.C. Schroeder, I. McCulloch, H.J. Bakker, J.R. Durrant, R.H. Friend, J. Phys. Chem. Lett. 4 (2013) 209.
[18] S.V. Rosokha, J.K. Kochi, Acc. Chem. Res. 41 (2008) 641.
[19] F.A. Cotton, N.F. Curtis, C.B. Harris, B.F.G. Johnson, S.J. Lippard, J.T. Mague, W.R. Robinson, J.S. Wood, Science 145 (1964) 1305.
[20] R.H. Cayton, M.H. Chisholm, J.C. Huffman, E.B. Lobkovsky, J. Am. Chem. Soc. 113 (1991) 8709.
[21] R.H. Cayton, M.H. Chisholm, J.C. Huffman, E.B. Lobkovsky, Angew. Chem., Int. Ed. 30 (1991) 862.
[22] R.H. Cayton, M.H. Chisholm, J. Am. Chem. Soc. 111 (1989) 8921.
[23] F.A. Cotton, C. Lin, C.A. Murrillo, J. Chem. Soc., Dalton Trans. (1998) 3151.
[24] F.A. Cotton, J.P. Donahue, C.A. Murillo, J. Am. Chem. Soc. 125 (2003) 5436.
[25] F.A. Cotton, J.P. Donahue, C.A. Murillo, L.M. Pérez, J. Am. Chem. Soc. 125 (2003) 5486.
[26] F.A. Cotton, C. Lin, C.A. Murillo, Acc. Chem. Res. 34 (2001) 759.
[27] M.H. Chisholm, A.M. Macintosh, Chem. Rev. 105 (2005) 2949.
[28] M.H. Chisholm, N.J. Patmore, Acc. Chem. Res. 40 (2007) 19.
[29] C.A. Murillo, Inorg. Chim. Acta. 424 (2015) 3.
[30] X. Xiao, C.Y. Liu, Q. He, M.J. Han, M. Meng, H. Lei, X. Lu, Inorg. Chem. 52 (2013) 12624.
[31] C.Y. Liu, X. Xiao, M. Meng, Y. Zhang, M.J. Han, J. Phys. Chem. C 117 (2013) 19859.
[32] Y. Shu, H. Lei, Y.N. Tan, M. Meng, X.C. Zhang, C.Y. Liu, Dalton Trans. 43 (2014) 14756.
[33] X. Xiao, M. Meng, H. Lei, C.Y. Liu, J. Phys. Chem. C 118 (2014) 8308.
[34] T. Cheng, M. Meng, H. Lei, C.Y. Liu, Inorg. Chem. 53 (2014) 9213.
[35] F.A. Cotton, J.P. Donahue, C. Lin, C.A. Murillo, Inorg. Chem. 40 (2001) 1234.
[36] F.A. Cotton, L.M. Daniels, J.P. Donahue, C.Y. Liu, C.A. Murillo, Inorg. Chem. 41 (2002) 1354.
[37] F.A. Cotton, C.Y. Liu, C.A. Murillo, X. Wang, Inorg. Chem. 42 (2003) 4619.
[38] F.A. Cotton, C.Y. Liu, C.A. Murillo, D. Villagrán, X. Wang, J. Am. Chem. Soc. 125 (2003) 13564.
[39] F.A. Cotton, C.Y. Liu, C.A. Murillo, D. Villagrán, X. Wang, J. Am. Chem. Soc. 126 (2004) 14822.
[40] F.A. Cotton, Z. Li, C.Y. Liu, C.A. Murillo, D. Villagrán, Inorg. Chem. 45 (2006) 767.
[41] F.A. Cotton, Z. Li, C.Y. Liu, C.A. Murillo, Inorg. Chem. 46 (2007) 7840.
[42] C.E.B. Evans, M.L. Naklicki, A.R. Rezvani, C.A. White, V.V. Kondratiev, R.J. Crutchley, J. Am. Chem. Soc. 120 (1998) 13096.
[43] D.E. Richardson, H. Taube, Inorg. Chem. 20 (1981) 1278.
[44] M.H. Chisholm, N.J. Patmore, J. Chem. Soc., Dalton Trans. (2006) 3164.
[45] M.J. Han, C.Y. Liu, P.F. Tian, Inorg. Chem. 48 (2009) 6347.
[46] B.S. Brunschwig, C. Creutz, N. Sutin, Chem. Soc. Rev. 31 (2002) 168.
[47] N.S. Hush, Prog. Inorg. Chem. 8 (1967) 391.
[48] N.S. Hush, Electrochim. Acta 13 (1968) 1005.
[49] R.A. Marcus, J. Chem. Phys. 24 (1956) 966.
[50] R.A. Marcus, N. Sutin, Biochim. Biophys. Acta 812 (1985) 811.
[51] L. Karki, H.P. Lu, J.T. Hupp, J. Phys. Chem. 100 (1996) 15637.
[52] J.T. Hupp, Y. Dong, R.L. Blackbourn, H. Lu, J. Phys. Chem. 97 (1993) 3278.
[53] S.F. Nelsen, M.D. Newton, J. Phys. Chem. A 104 (2000) 10023.
[54] D.M. D'Alessandr, P.H. Dinolfo, J.T. Hupp, P.C. Junk, F.R. Keene, Eur. J. Inorg. Chem. 2006 (2006) 772.
[55] B.S. Brunschwig, C. Creutz, N. Sutin, Coord. Chem. Rev. 177 (1998) 61.
[56] Y.K. Shin, B.S. Brunschwig, C. Creutz, N. Sutin, J. Phys. Chem. 100 (1996) 8157.
[57] G.T. Burdzinski, M.H. Chisholm, P.-T. Chou, Y.-H. Chou, F. Feil, J.C. Gallucci, Y. Ghosh, T.L. Gustafson, M.-L. Ho, Y. Liu, R. Ramnauth, C. Turro, Proc. Natl. Acad. Sci. U.S.A 105 (2008) 15247.
[58] C. Lin, J.D. Protasiewicz, E.T. Smith, T. Ren, Inorg. Chem. 35 (1996) 6422.
[59] H.M. McConnell, J. Chem. Phys. 35 (1961) 508.
[60] C. Creutz, M.D. Newton, N. Sutin, J. Photochem. Photobiol. A 82 (1994) 47.
[61] A.J. Distefano, J.F. Wishart, S.S. Isied, Coord. Chem. Rev. 249 (2005) 507.
[62] A.R. Rezvani, C. Bensimon, B. Cromp, C. Reber, J.E. Greedan, V.V. Kondratiev, R.J. Crutchley, Inorg. Chem. 36 (1997) 3322.
[63] S.V. Rosokha, D.-L. Sun, J.K. Kochi, J. Phys. Chem. A 106 (2002) 2283.
[64] N. Sutin, Prog. Inorg. Chem. 30 (1983) 441.
[65] T. Ito, T. Hamaguchi, H. Nagino, T. Yamaguchi, H. Kido, I.S. Zavarine, T. Richmond, J. Washington, C.P. Kubiak, J. Am. Chem. Soc. 121 (1999) 4625.
[66] C. Lambert, G. Nöll, J. Am. Chem. Soc. 121 (1999) 8434.
[67] S.F. Nelsen, Chem. Eur. J. 6 (2000) 581.
[68] F. Barigelletti, L. Flamigni, M. Guardigli, A. Juris, M. Beley, S. Chodorowski-Kimmes, J.-P. Collin, J.-P. Sauvage, Inorg. Chem. 35 (1996) 136.